

Quantum virial expansion approach to thermodynamics of ^4He adsorbates in carbon nanotube materials: Interacting Bose gas in one dimension

Antonio Šiber*

Institute of Physics, P.O. Box 304, 10001 Zagreb, Croatia

(Received 15 November 2002; revised manuscript received 21 January 2003; published 30 April 2003)

I demonstrate that ^4He adsorbates in carbon nanotube materials can be treated as one-dimensional interacting gas of spinless bosons for temperatures below 8 K and for coverages such that all the adsorbates are in the groove positions of the carbon nanotube bundles. The effects of adsorbate-adsorbate interactions are studied within the scheme of the virial expansion approach. The theoretical predictions for the specific heat of the interacting adsorbed gas are given.

DOI: 10.1103/PhysRevB.67.165426

PACS number(s): 68.43.De, 68.65.-k, 51.30.+i, 65.80.+n

I. INTRODUCTION

The adsorption of gases in nanotube-based materials has been recently a subject of considerable interest and many theoretical and experimental studies focused on this phenomenon have been reported.¹⁻¹² The interest in the subject stems partially from the possibility to use these materials as efficient gas containers for hydrogen storage.¹³ Another reason for the interest is that the nanotube materials provide a very specific potential-energy environment for the gas atoms and molecules. In particular, the nature of this environment is such that it reduces the effective dimensionality of adsorbates^{8,9} which at sufficiently low temperatures behave as one-dimensional (1D) gases. This provides an excellent opportunity to study the interactions in the 1D gas. The problem of N particles interacting mutually via binary interaction potentials in one dimension has been thoroughly investigated in the literature and there exist exact quantum and classical solutions for very specific functional forms of the interaction potential.¹⁴⁻¹⁷ The aim of this paper is to investigate a realistic system in which the adsorbate atoms (molecules) interact with a relatively complicated binary potential that is attractive at large and repulsive at short interadsorbate separations.¹⁸

The outline of this paper is as follows. In Sec. II, the behavior of a single atom adsorbed on the surface of a bundle of single-wall carbon nanotubes (SWCNT's) is discussed. The range of temperatures in which the isolated adsorbates exhibit effective one-dimensional behavior is discussed for ^4He atoms. In Sec. III the calculation of a second virial coefficient for the interacting gas in one dimension is briefly outlined. A fully quantal approach is followed since the gas of interest is composed of ^4He atoms for which quantum effects are essential. In Sec. IV the specific heat of adsorbed He gas is predicted and the effects of He-He interactions are discussed. The results obtained are compared with those for exactly solvable models^{15,16} and qualitative agreement is found. The calculation of specific heat in combination with experiments, some of them quite recently reported,^{19,20} is expected to yield additional insight into the thermodynamics of the adsorbed gas. In Sec. V, the influence of the corrugation of the nanotube (which is neglected in Secs. II-IV) and sample inhomogeneities on the thermody-

namics of adsorbed gas is thoroughly discussed. Section VI concludes the paper and summarizes the main results of the present work.

II. BEHAVIOR OF ISOLATED ^4He ATOMS ADSORBED ON THE SURFACE OF A BUNDLE OF SWCNT's

Although there is still ongoing discussion^{1-4,9,10} concerning the preferable adsorption sites for He atoms in SWCNT materials, the experimental information¹⁻³ combined with the theoretical considerations⁹⁻¹¹ suggests that individual He atoms are predominantly adsorbed in the groove positions on the SWCNT's bundle surface. If the number of He atoms adsorbed in the sample is very large, then one can expect that the He atoms will also occupy other positions on the bundle surface. This point is discussed in Sec. III.

Quantum states of ^4He atoms adsorbed in the groove positions of an infinitely long bundle made of (10,10) SWCNT's have been discussed in Ref. 9. It was found that the low-energy part of the ^4He excitation spectrum exhibits a typical 1D behavior with characteristic $1/\sqrt{E}$ singularities present in the density of states, $g(E)$. The density of states does not exhibit gaps which is a consequence of the neglect of the corrugation of the carbon nanotube. In this approximation there are no potential barriers for the adsorbate motion along the groove. The severeness of this approximation and its influence on the results presented is discussed in Sec. V. In Fig. 1, the low-energy part of the ^4He density of states per unit length of the groove is presented, which was calculated as described in Ref. 9, i.e., the three-dimensional Schrödinger equation was numerically solved to yield the complete set of bound states. As can be seen in Fig. 1, all the excitations with energies between -22.7 meV and -18.88 meV pertain to essentially one-dimensional ^4He atoms. The excitations in this regime of energies represent the activated, free motion of ^4He atoms along the groove characterized by a 1D wave vector K_y (the y axis is oriented along the groove), as discussed in Ref. 9. The transverse profile (in the xz plane, perpendicular to the groove direction) of the ^4He wave function is the same for all these excitations and can be represented by a narrow, Gaussian-like 2D function [see Fig. 4(a) in Ref. 9].

At -18.88 meV, another band of states becomes available to the isolated adsorbates. In this band, the transverse

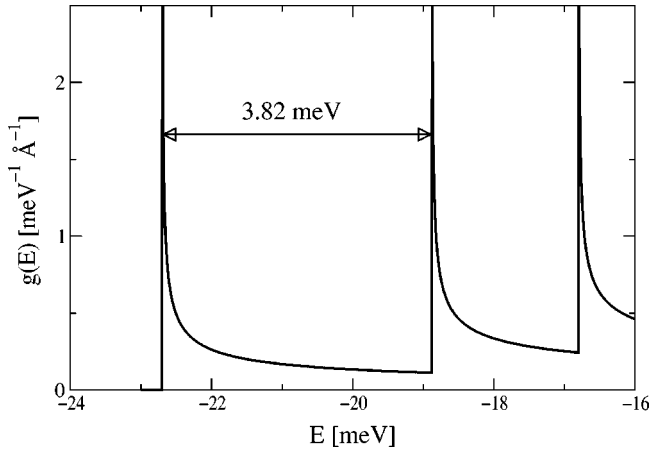


FIG. 1. Density of states per unit length of the groove of a single ^4He atom adsorbed in the groove of a bundle made of (10,10) SWCNT's. The low-energy portion of the density of states is displayed.

profile of the ^4He wave function is different from the ground-state profile [see Fig. 4(b) in Ref. 9]. As discussed in Ref. 9, the population of higher (excited) bands causes transition from the effectively 1D behavior of ^4He atoms to 2D, and eventually, 3D behavior.

For the purposes of this work, it is sufficient to note that the separation between the lowest 1D band and the first excited band is quite large (3.82 meV) which immediately suggests that the higher bands are poorly populated in a significant range of temperatures. The width of this temperature range can be evaluated from the known density of states. The total density of states can be represented as a sum of the lowest band density of states, $g_0(E)$, and the density of states representing all other transverse excitations, g_a ,

$$g(E) = g_0(E) + g_a(E). \quad (1)$$

The lowest band density of states per unit length of the groove is given by⁹

$$g_0(E) = \sqrt{\frac{2m}{\hbar^2}} \frac{1}{2\pi} \frac{\Theta(E - E_\Gamma)}{\sqrt{E - E_\Gamma}}, \quad (2)$$

where the mass of the adsorbate is m , $E_\Gamma = -22.7$ meV is the ground-state energy, and Θ is the Heaviside function. The total number of adsorbates, N , is given by

$$N = L \int_{E_\Gamma}^{\infty} g(E) f(E, T) dE, \quad (3)$$

where L is the total length of the groove, and the Bose-Einstein distribution function is given by

$$f(E, T) = \frac{1}{\exp\left(\frac{E - \nu}{k_B T}\right) - 1}. \quad (4)$$

Here, k_B is the Boltzmann constant, T is the temperature, and ν is the chemical potential. The number of adsorbates in the lowest band, N_0 , can be calculated as

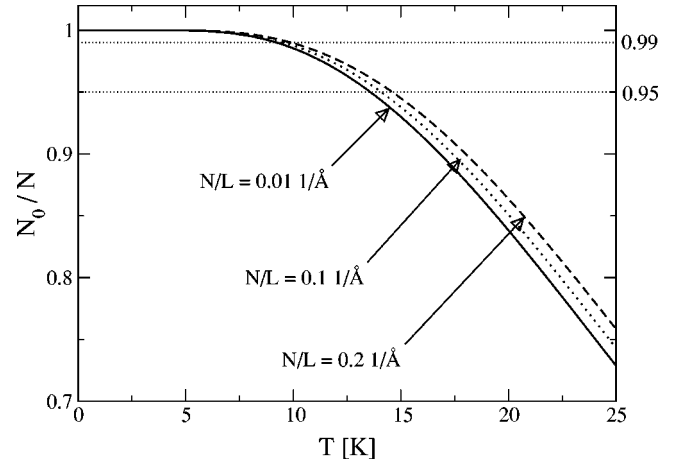


FIG. 2. Ratio of the number of ^4He atoms in the lowest 1D band and the total number of ^4He atoms (N_0/N) as a function of temperature and for three different linear densities. Thick full line: $N/L = 0.011/\text{\AA}$. Thick dashed line: $N/L = 0.11/\text{\AA}$. Thick dotted line: $N/L = 0.21/\text{\AA}$. Two thin dotted lines represent the 0.99 and 0.95 values of the ratio.

$$N_0 = L \int_{E_\Gamma}^{\infty} g_0(E) f(E, T) dE, \quad (5)$$

once the chemical potential has been determined from Eq. (3).

In Fig. 2, I plot the ratio N_0/N as a function of temperature and for three different linear densities of adsorbates, n , $n = N/L$. From this figure one can conclude that the *non-interacting* ^4He gas can be treated as effectively being 1D for temperatures smaller than about 8 K (13 K) since for these temperatures more than 99% (95%) of ^4He atoms occupy the lowest-energy band.

III. VIRIAL EXPANSION APPROACH TO TREATING THE INTERACTING GAS IN ONE DIMENSION

The approach to be presented here assumes that all the adsorbed atoms are in the groove positions on the bundle surface. Thus, the approach cannot be applied to the situations where the number of adsorbates is so large that other positions on the bundle surface become occupied by the adsorbates. One could envisage the situation where a very large number of atoms is adsorbed on the bundle surface. From this phase, one could get to the phase where all the adsorbates are exclusively in the groove positions by desorbing all the atoms which are not in groove positions. These atoms are more weakly bound than those in the grooves⁹ and will desorb from the sample at lower temperatures. This fact enables the experimental realization of the 1D phase of interest to this work. Similar arguments can be applied to 1D heavy adsorbate phases studied in Ref. 12.

The virial expansion approach to treating the imperfect (interacting) quantum gas is well known²¹⁻²³ and in this section it will be only briefly outlined with reference to a quantum gas in one dimension. The basic idea of the virial expansion approach is to represent the so-called gas spreading pressure, ϕ , as a power series of the gas density, n ,

$$\beta\phi = \sum_{l=1}^{\infty} B_l(L, \beta) n^l. \quad (6)$$

Here, $\beta = 1/k_B T$ and coefficients B_l are the virial coefficients. The virial coefficients can be obtained by comparing the expansion of the gas spreading pressure in the power series of fugacity, $z = \exp(\beta\mu)$,

$$\beta\phi = \frac{1}{L} \ln Q(z, \beta, L) = \sum_{l=1}^{\infty} b_l(L, \beta) z^l \quad (7)$$

with the expansion in Eq. (6). b_l is the l th cluster integral obtained as the coefficient in the power-series expansion of the logarithm of the grand partition function, Q , in terms of fugacity. Since the grand partition function is given by

$$Q(z, L, \beta) = \sum_{l=0}^{\infty} Z_l(L, \beta) z^l, \quad (8)$$

where Z_l are the quantum partition functions for l particles, the formulas for cluster integrals can be obtained by comparing the expansions in Eqs. (7) and (8). The general form of b_l is given in Ref. 21. For the first two cluster integrals one has

$$b_1 = \frac{Z_1}{L},$$

$$b_2 = \frac{Z_2 - \frac{1}{2} Z_1^2}{L}. \quad (9)$$

Eliminating z from Eqs. (6) and (7) by expressing it in terms of linear density n yields the relation between the virial coefficients and cluster integrals. Using Eq. (9), one can obtain the relations between virial coefficients and quantum partition functions. Explicitly, for the first and second virial coefficient one has

$$B_1 = 1,$$

$$B_2 = L \left(\frac{1}{2} - \frac{Z_2}{Z_1^2} \right). \quad (10)$$

The quantum expression for the partition function of N particles in one dimension is

$$Z_N = \int dy_1 \cdots dy_N \sum_{\alpha} \Psi_{\alpha}^*(y_1, \dots, y_N)$$

$$\times \exp[-\beta H(p_1, \dots, p_N, y_1, \dots, y_N)]$$

$$\times \Psi_{\alpha}(y_1, \dots, y_N), \quad (11)$$

where p_i and y_i , $i = 1, \dots, N$, represent 1D momenta and coordinates of the N gas particles, respectively. The dynamics of N gas particles is described by the Hamiltonian $H(p_1, \dots, p_N, y_1, \dots, y_N)$. A complete set of quantum states describing N particles is denoted by $\{\alpha\}$. The wave functions Ψ_{α} are assumed to be properly normalized and symmetrized according to the statistics satisfied by the gas

particles. It is easy to show²¹⁻²³ that the partition function for one 1D spinless particle is given by

$$Z_1 = \frac{L}{\lambda}, \quad (12)$$

where λ is the thermal wavelength, $\lambda = \sqrt{2\pi\hbar^2\beta/m}$. Since I consider ⁴He atoms, the consideration of spinless particles suffices. As shown by the authors of Ref. 21, the spin degrees of freedom can be considered (if needed) after the spinless problem has been solved. In the problem of spinless particles (anti)symmetrization of the wave function is performed solely in the coordinate space. All expressions which follow do not consider the spin degrees of freedom.

For the calculation of the second virial coefficient, B_2 , given by Eq. (10), one needs to calculate the partition function for two-interacting particles. This is an easy task when the corrugation of the nanotubes can be neglected, since in that case the interacting two-body problem can be reduced to free motion of the center of mass and the relative motion representing a particle of reduced mass $\mu = m/2$ in an external potential.²¹⁻²⁴ The motion of the center-of-mass can be represented by a wave function for the free particle of mass $2m$, $\exp(ik_{cm}Y)/\sqrt{L}$, where k_{cm} is the wave vector of the center-of-mass motion and Y is the center-of-mass coordinate, $Y = (y_1 + y_2)/2$. The relative motion can be described by a wave function of relative coordinate, $y = y_1 - y_2$, which is denoted by $\xi_c(y)$, and which satisfies the 1D Schrödinger equation

$$\left[-\frac{\hbar^2}{2\mu} \frac{d^2}{dy^2} + v(|y|) \right] \xi_c(y) = \epsilon_c \xi_c(y). \quad (13)$$

The binary potential representing an interaction between the two gas particles is denoted by $v(|y|) = v(|y_1 - y_2|)$. The set of “relative” quantum states is denoted by $\{c\}$. This set consists of a finite number of bound states denoted by $\{b\}$, and the continuum of states which can be numbered according to the wave vector k associated with the motion of the particle with reduced mass in the region where the interaction vanishes (large y). The energy of the quantum state $|c\rangle$ is denoted by ϵ_c . Relative wave functions behave in the asymptotic regime ($y \rightarrow \infty$) as

$$\xi_k(y) \rightarrow \frac{1}{\sqrt{L}} \sin[ky + \eta(k)],$$

$$\xi_b(y) \rightarrow 0. \quad (14)$$

The 1D phase shifts, which are nonvanishing due to the presence of the interaction potential v , are denoted by $\eta(k)$.

The partition function for the two *noninteracting* particles [$v(|y|) = 0$] in one dimension can be calculated without invoking Y and y coordinates. Its form results solely from the requirement of the (anti)symmetrization of the total wave function. Explicitly,

$$Z_2^{(0)} = \frac{Z_1^2}{2} \pm \frac{L}{2\sqrt{2}\lambda}, \quad (15)$$

where the upper(lower) sign is for a spinless boson (fermion) gas. The second virial coefficient for the *noninteracting* gas is thus

$$B_2^{(0)} = \mp \frac{\lambda}{2\sqrt{2}}. \quad (16)$$

The superscripts (0) in Eqs. (15) and (16) indicate that the expressions correspond to the noninteracting quantum gas. As often noted in the literature,^{22,23} the finite value of the $B_2^{(0)}$ coefficient for noninteracting quantum gas reflects the so-called statistical attraction for bosons [negative $B_2^{(0)}$] and statistical repulsion for fermions [positive $B_2^{(0)}$, see Eq. (6)]. The expression for $B_2^{(0)}$ should be compared with Eq. (3.15) of Ref. 21 which pertains to noninteracting gas in two dimensions.

The second virial coefficient can be calculated as

$$B_2 = B_2^{(0)} + \lambda \sqrt{2} \sum_c \{ \exp[-\beta \epsilon_c^{(0)}] - \exp(-\beta \epsilon_c) \}, \quad (17)$$

where $\epsilon_c^{(0)}$ is the set of “relative” energies for two noninteracting particles. Equation (17) has been obtained by performing integration over the center-of-mass coordinate in the expression for the partition function of the two interacting particles, Z_2 [Eq. (11)].

The formula for B_2 which is convenient for numerical implementation can be obtained by replacing the summation over $\{c\}$ in Eq. (17) with two summations, one going over the bound states, $\{b\}$, and the other over the continuum states, $\{k\}$. One can pass from the sum over states $\{k\}$ to the integral over the wave vector k by introducing the density of states in k space, which can be obtained from the 1D phase shifts, $\eta(k)$.²¹ I finally obtain

$$B_2(\beta) = B_2^{(0)}(\beta) - \lambda \sqrt{2} \sum_b \exp(-\beta \epsilon_b) - \frac{\lambda \sqrt{2}}{\pi} \int_0^\infty \frac{d\eta(k)}{dk} \exp\left(-\beta \frac{\hbar^2 k^2}{2\mu}\right) dk, \quad (18)$$

where the dependence of the virial coefficient on the temperature (or β) is emphasized. This formula is very similar to the one obtained for 2D and 3D gases, although the numerical factors (such as $\sqrt{2}$) and units of B_2 (in one dimension, B_2 has units of length since the linear density has units of inverse length) are different, depending on a dimensionality of the problem. It should also be noted that since the problem involves only one dimension, one does not obtain azimuthal quantum numbers which occur in the treatments of interacting gases in two and three dimensions as a consequence of the central symmetry of the binary potential.

The evaluation of Eq. (18) requires the calculation of 1D phase shifts which depend on the binary potential, v . The interaction between the two He atoms in the otherwise empty space is known to great precision.¹⁸ However, the effective interaction between the two He atoms positioned in the vicinity of a third polarizable body is different from the free

space He-He interaction.²⁵ In the case of interest to this work, the two He atoms are surrounded by two SWCNT's and the polarization induced in the SWCNT's will modify the He-He interaction. While the polarization-induced effects on the binary potential can be calculated for atoms physisorbed on a crystalline surface,²⁵ the analogous calculation for the very specific geometry of the nanotube bundle is certainly more difficult. It is interesting to note here, that Vidali and Cole²⁶ found that the measurements of specific heat of He overlayers on graphite²⁷ can be more accurately reproduced by the effective He-He potential which is 15% shallower from the free-space He-He potential. They attribute this effect to the screening of He-He interaction by the substrate. The treatment of Vidali and Cole²⁶ was also based on quantum virial expansion. In another study,²⁸ more related to the system considered here, the authors found that the interaction between two He atoms adsorbed in the interstitial channels of SWCNT's has a well depth which is 28% shallower with respect to the free-space interaction. The groove adsorption represents a situation which is “somewhere in between” the adsorption on planar graphite and in SWCNT's interstitial channels.

In the following calculations, the He-He interaction will be described by free-space potential suggested recently by Janzen and Aziz,¹⁸ but I also consider the scaled potential obtained from the free-space interaction by simple multiplication with a factor of 0.785. Thus, the scaled potential has a well depth which is 21.5% smaller from the well depth of the free-space potential. This number was obtained as a simple arithmetic mean of the well depth reductions found for adsorption on planar graphite²⁶ and in interstitial channels of SWCNT's.²⁸ The assumed reduction of the well depth is quite close to the numerical estimate in Ref. 28 (24%). The exact value of the scaling factor used should not be taken too seriously because the substrate-induced contributions to the potential cannot be modeled by a simple scaling of the free-space potential.²⁵ The scaled potential was introduced simply to examine the effects of the details of interaction potential on the thermodynamics of adsorbed gas. Additionally, to obtain the effective potential in one dimension, the 3D potential should be averaged over the 2D cross sections of the adsorbate probability density.^{26,29} However, since the cross section of the lowest band states is rather small, and in light of the uncertainties of the substrate-mediated forces, such a procedure has not been performed.

SAPT1 potential supports one weakly bound state in one dimension, representing a ^4He dimer with an energy of $\epsilon_0 = -0.16 \mu\text{eV}$. This state, being so weakly bound, is extremely extended in a relative coordinate.^{30,31} The bound state energy in one dimension is significantly smaller than the one obtained by Siddon and Schick in a 2D treatment,²¹ which is in accord with the existing literature.³⁰ The scaled SAPT1 potential does not support bound states. The 1D phase shifts and their derivatives with respect to the relative wave vector were calculated by numerically solving the Schrödinger equation using an algorithm quite similar to the one described in Ref. 32.

In Fig. 3, the calculated values of a second virial coefficient are presented. The full line corresponds to calculations

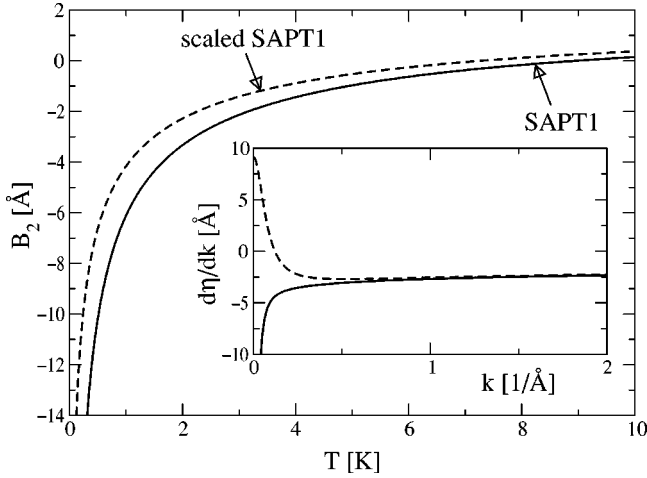


FIG. 3. Second virial coefficient for 1D ${}^4\text{He}$ gas as a function of temperature. Full line: Quantum calculation with the SAPT1 potential. Dashed line: Quantum calculation with the scaled SAPT1 potential (see text). Inset: Phase-shift derivatives, $d\eta(k)/dk$, corresponding to the SAPT1 potential (full line) and the scaled SAPT1 potential (dashed line).

with the He-He potential suggested in Ref. 18 (SAPT1), while the dashed line corresponds to calculations using the scaled SAPT1 potential. The behavior of the second virial coefficient with temperature is qualitatively similar to the one obtained for ${}^4\text{He}$ adsorbates on graphite (2D problem) in Ref. 21. There is, however, one important difference. The ideal gas term, B_2^0 , reflecting the purely quantum effect of gas statistics, decays with temperature as $\sqrt{1/T}$ in one dimension, and as $1/T$ in two dimension.²¹ Thus, the approach of a second virial coefficient to its classical value as the temperature increases is slower in one than in two dimensions. In the inset of Fig. 3 the derivatives of the phase shifts, $d\eta(k)/dk$, are plotted as a function of relative wave vector k . Note that the phase-shift derivatives become negative and nearly constant for large relative energies (wave vectors). This is a consequence of a strongly repulsive potential at short distances (hard core). Note also that the phase shifts of the two potentials are very different for small wave vectors, and thus one could expect that the two potentials produce quite different thermodynamical quantities. However, the very different behavior of the phase shifts is a consequence of the fact that the SAPT1 potential supports a weakly bound state whereas the scaled SAPT1 potential does not. Thus, in the evaluation of Eq. (18) one has to properly account for the bound state which exists in the case of the SAPT1 potential. This “extra” term for the SAPT1 potential makes the thermodynamical quantities derived from the two potentials quite similar, although the derivatives of the phase shifts are very different. This fact has been discussed for the interacting gas in two dimensions^{33,34} in connection with Levinson’s theorem,^{24,35} which relates the phase shift at zero momentum to the number of bound states. It was found³³ that a proper account of both the continuum and bound states eliminates discontinuities in thermodynamic properties whenever an extra bound state appears with the small change of the parameters of

interaction potential. In the present calculation a similar effect is found in one dimension.

IV. SPECIFIC HEAT OF ADSORBED ${}^4\text{He}$ GAS

The specific heat of interacting quantum gas can be calculated from the set of virial coefficients.^{22,23} I assume that the dominant contribution to the specific heat comes from the second virial coefficient. Thus, the results are applicable to a restricted range of adsorbate concentrations and temperatures. The range of validity of this approximation can be estimated from a calculation of higher virial coefficients, which is a difficult task, or from direct comparison with experiments, as has been done for ${}^4\text{He}$ adsorbates on graphite in Refs. 21 and 36. Experiments dealing primarily with the specific heat of adsorbates in carbon nanotube materials have not been reported yet and those which detected the signature of the adsorbed gas in the overall specific heat of the sample were focused on the specific heat of clean nanotube materials.^{19,20}

The isosteric specific heat is given as²¹

$$\frac{C}{Nk_B} = \frac{1}{2} - n\beta^2 \frac{d^2 B_2}{d\beta^2}. \quad (19)$$

The second term in Eq. (19) can be calculated from Eq. (18) as

$$n\beta^2 \frac{d^2 B_2}{d\beta^2} = n\lambda \sqrt{2} \left[\frac{1}{16} + \frac{S_0 + I_0}{4} + \beta(S_1 + I_1) - \beta^2(S_2 + I_2) \right], \quad (20)$$

where

$$S_n = \sum_b \epsilon_b^n \exp(-\beta \epsilon_b), \quad (21)$$

$$I_n = \frac{1}{\pi} \left(\frac{\hbar^2}{2\mu} \right)^n \int_0^\infty k^{2n} \frac{d\eta(k)}{dk} \exp\left(-\frac{\hbar^2 k^2 \beta}{2\mu}\right) dk. \quad (22)$$

The expression for the term in Eq. (20) representing a deviation of the specific heat from its ideal value (where the interadsorbate interactions are neglected) is different from the corresponding expression one would obtain in a 2D treatment. The 2D expression²¹ does not contain a term proportional to λ and independent of the interadsorbate interaction potential [$1/16$ in Eq. (20)]. The reason for this is that in two dimensions, the noninteracting value of B_2 , $B_2^{(0)}$ is proportional to β [$B_2^{(0)} = -\lambda^2/4$],²¹ and therefore, its second derivative with respect to β vanishes. In the 1D case, $B_2^{(0)} \propto \sqrt{\beta}$ [see Eq. (16)] and $d^2 B_2^{(0)}/d\beta^2 \propto \beta^{-3/2}$. This fact alone suggests that the specific heats of a dilute, interacting boson gas in one and two dimension may be qualitatively different.

In Fig. 4 I plot the quantity $-\beta^2 d^2 B_2/d\beta^2$. The full (dashed) line represents the calculation with the SAPT1 (scaled SAPT1) potential. Obviously, both potentials produce similar deviations. The calculation with the scaled SAPT1 potential yields somewhat smaller effects of interactions on the specific heat, which is plausible since the scaled SAPT1

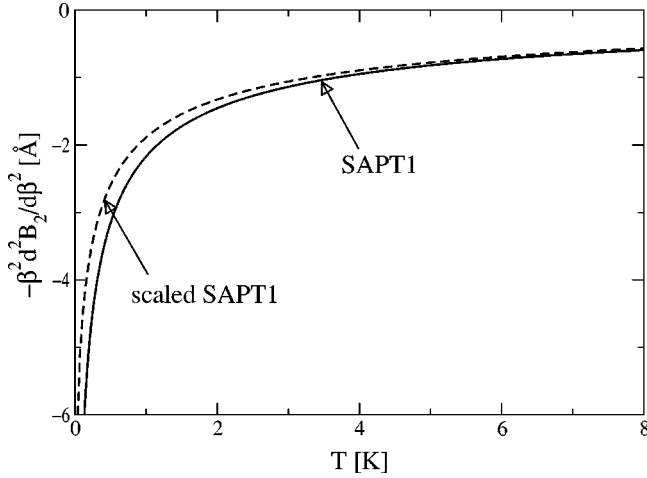


FIG. 4. Deviation of the specific heat per unit linear density ($-\beta^2 d^2 B_2 / d\beta^2$) from its ideal value, Eq. (19). Full line: Calculation with the SAPT1 potential. Dashed line: Calculation with the scaled SAPT1 potential.

potential is weaker than the SAPT1 potential. An important observation is that the deviation of specific heat from its ideal value is *negative* for a 1D boson gas, i.e., the inclusion of interactions reduces the specific heat of the adsorbed 1D gas. For a 2D spinless boson gas considered in Ref. 21, the deviation was found to be *positive*. The observed difference between 1D and 2D results is a consequence of both the nonvanishing second derivative of the ideal term [$B_2^{(0)}(\beta)$] with respect to β , and nonexistence of azimuthal degrees of freedom in the 1D treatment of the problem.

Finally, in Fig. 5, I plot the specific heat of the interacting ^4He gas adsorbed in grooves of SWCNT bundles for three different linear densities. The full (dashed) lines represent the calculation with the SAPT1 (scaled SAPT1) potential. Obviously, for denser gas, the specific heat is more strongly influenced by the interactions, and deviates more from the ideal (noninteracting) 1D value (compare with Fig. 6 of Ref.

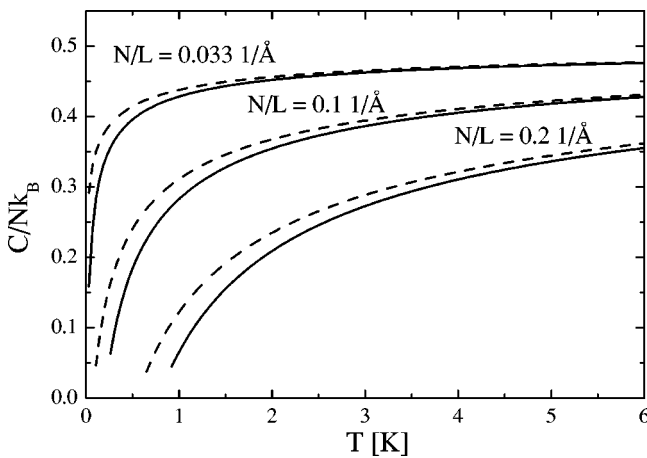


FIG. 5. Specific heat of ^4He gas adsorbed in the grooves of SWCNT bundles for three different linear densities (0.033 $1/\text{\AA}$, 0.1 $1/\text{\AA}$, and 0.2 $1/\text{\AA}$). Full line: Calculation with the SAPT1 potential. Dashed line: Calculation with the scaled SAPT1 potential.

9). It can also be inferred from Fig. 5 that the description of thermodynamics of the adsorbed gas in terms of the second virial coefficient only breaks down at very low temperatures where such an approach yields negative specific heat. These temperatures can be considered as the lower limits for the application of the present approach. For higher densities, the lower-temperature limits obviously increase, in agreement with Eq. (19), and the presented virial expansion approach breaks down at higher temperatures. Note that the upper temperature for which the specific heat was calculated is 6 K. Above that temperature the higher bands start to contribute to the specific heat as discussed in Sec. II and Ref. 9. Although the number of particles in higher bands is very small at 6 K (see Fig. 1), the derivative of internal energy with respect to temperature (specific heat) is very sensitive even to very small occupations of the higher bands and this causes the increase of the specific heat observed for a very dilute gas.

It is now of interest to compare the obtained results with those of exactly solvable 1D many-particle models. In particular, for the gas of bosons in one dimension interacting via a repulsive δ -function potential, Lieb and Liniger have demonstrated that the energy spectrum of such a gas is identical to the spectrum of a noninteracting Fermi gas.^{15,16} The same was found in the model of Girardeau¹⁷ for 1D bosons interacting with the binary hard-core potentials of finite radius. The Fermi energy E_F of the corresponding 1D Fermi gas is given as

$$E_F = \frac{\hbar^2 k_F^2}{2m} = \frac{\hbar^2 \pi^2}{2m} n^2, \quad (23)$$

where $k_F = \pi N/L = \pi n$ is the Fermi wave vector. This mapping (interacting Bose gas vs noninteracting Fermi gas) allows us to easily predict the specific heat of the impenetrable 1D Bose gas. Thus, at temperatures much smaller than the Fermi temperature, $T_F = E_F/k_B$,

$$C_V(T \ll T_F) \propto T, \quad (24)$$

while at temperatures much larger than the Fermi temperature, the specific heat reduces to its classical equipartition value

$$\frac{C_V(T \gg T_F)}{Nk_B} \rightarrow \frac{1}{2}. \quad (25)$$

The linear temperature dependence of the specific heat [Eq. (24)] can be also interpreted as a signature of long-wavelength compression waves of the 1D Bose gas (sound), and is thus also expected in a gas of 1D bosons interacting with more complex forces. This is a collective effect and is obviously outside of the scope of the second-order virial expansion, treating only the two-body collisions. On the other hand, the classical equipartition value of specific heat [Eq. (25)] is obtained also by the present approach at high temperatures [Eq. (19) and Fig. 4]. The temperature separating the two characteristic behaviors in Eqs. (24) and (25) is roughly given by the Fermi temperature of the equivalent noninteracting Fermi gas, which is proportional to the square

of linear density [Eq. (23)]. Thus, for denser Bose gases, the interval of temperatures in which the specific heat is significantly smaller than one-half is larger. This is again in agreement with the results presented in Fig. 5.

V. THE EFFECT OF THE CORRUGATION OF CARBON NANOTUBES AND SAMPLE INHOMOGENEITIES

The results presented in this paper are based on an idealized representation of the SWCNT materials. In particular, it is assumed that SWCNT bundles are infinitely long, straight, and smooth, which is certainly not the case in real materials, and the bundles wiggle on large length scales. The discreteness of the nanotube results in the corrugation of the potential experienced by adsorbates, which is not accounted for in the present approach. The influence of the corrugation of the potential confining the He atom to the interstitial channel of the bundle composed of (10,10) carbon nanotubes was studied in Ref. 11. A model potential was used which enabled an easy examination of effects induced by the potential details. A substantial effect of the corrugation on the density of states of a single He atom was predicted. In particular, for the lowest band of states, a mass enhancement factor of 2.37 was calculated. Another study⁶ predicted a mass enhancement factor of 1.3. The large difference between these factors predicted by the two studies can be attributed to the larger separation of the tubes (by 0.1 Å) adopted in Ref. 6 with respect to Ref. 11. For comparison, the mass enhancement factor for ⁴He adsorbed on graphite was found to be only 1.06.²⁶ For an interstitial channel surrounded by three (17,0) nanotubes, the authors of Ref. 6 found that a change in the intertube separation by 0.1 Å changes the effective mass of ⁴He by a factor of 2.

It is quite remarkable that a small change in the intertube separation results in a very large change of the band structure of adsorbates. A similar sensitivity of the adsorbate bound states on the interaction potential was found in Ref. 9 for the groove adsorption. The details of the interaction potential are “magnified” in the spatially restricted regions of the interstitial channel and the groove, and the band structure of adsorbates is much more affected by the potential details when compared with the adsorption on planar graphite. Thus, in order to assess the effect of the corrugation on the calculations presented in this paper, one would need to know the intertube separation distance to a precision better than at least 0.05 Å. Note that the groove region is at the surface of the bundle where the relaxation effects can be expected and the separation between the tubes surrounding the groove needs not to be the same as the separation between the two tubes in the interior of the bundle. Additionally, one would have to know the He single tube potential with great accuracy. Even then, the calculation of the corrugation of the potential would require knowledge of the alignment of the two tubes surrounding the groove. It is very likely that this arrangement is not the same for all the grooves on the bundle surface. Furthermore, if the two tubes surrounding a groove are not of the same symmetry, the corrugations of the two tubes are not necessarily commensurate and the total poten-

tial for the groove adsorption cannot be written as a Fourier series.

All the mentioned complications are not present for the adsorption on planar graphite. In that case, a fairly reliable potential can be constructed³⁶ and written as a 2D Fourier series. However, even the inclusion of periodic corrugation in the formalism of quantum virial expansion is not straightforward. The basic reason for this is that the two-body Schrödinger equation in the textured potential background no longer separates into the two equations describing the motion of the center of mass and the relative motion. For the adsorption of He on graphite, Guo and Bruch²⁹ devised a perturbation treatment in which the two-body cluster integral is written as an expansion in powers of the Fourier amplitudes of the atom-substrate potential. They also presented the results for the second virial coefficient in which the corrugation effects were treated up to second order of the perturbation series. Another study dealing with the problem³⁷ started from the tight-binding Hamiltonian and He atoms localized on particular adsorption sites. A series of approximations and simplifications was needed to obtain the formula for the second virial coefficient which is amenable to evaluation.

It is clear from the discussion in this section that a reliable calculation of the second virial coefficient with the effects of the corrugation included is not possible at present, mainly because the relevant potential is not known with sufficient precision. Additionally, aperiodic corrugation has not been treated in the literature in this context. However, a simple estimate of the corrugation effects is possible if we represent the adsorbate as a particle with the effective mass. Such a representation of the corrugation effects is adequate for excitations with small velocity, i.e., for the states located around the center of the 1D Brillouin zone. The mass enhancement for the groove adsorption can be expected to be somewhere between 1.06 (planar graphite) and 2.37 (interstitial channel). The quantity $-\beta^2 d^2 B_2 / d\beta^2$ was calculated using Eqs. (20)–(22), the scaled SAPT1 potential, and the effective He mass equal to $M^* = 1.3M_{\text{He}} = 5.2$ amu. At $T = 1$ K (5 K), its value was found to be -1.69 Å (-0.52 Å). This should be compared with the values obtained in Fig. 4. In particular, at $T = 1$ K (5 K) the values obtained using the free mass of ⁴He are -1.92 Å (-0.77 Å). Thus, the reflection of the corrugation effects on the specific heat can be significant, but the overall trends, at least in the model of renormalized mass, are the same. For strongly corrugated potentials, it may be more sensible to use the bandwidth for the characterization of the effects of corrugation rather than the curvature of dispersion curves at small wave vectors.³⁸

The influence of other bundles on the atoms adsorbed in a groove of a particular bundle is neglected. This approximation obviously breaks down if two bundles touch each other. At these points, the adsorbates move in a potential very much influenced by both bundles in question, which may be significantly different from the potential of a single, infinitely long and straight bundle I used in the calculations. For the adsorption of ⁴He on graphite,^{27,39} it was argued⁴⁰ that the presence of long-range inhomogeneities in the graphite may act as a trap and induce the Bose-Einstein condensation of

the adsorbed gas. The same experiments were later explained in terms of the virial expansion approach²¹ by assuming a perfect graphite substrate. Nevertheless, a possible substantial influence of the sample inhomogeneities on the thermodynamics of the adsorbed gas cannot be *a priori* ruled out. This is expected to be more important at low temperatures where the adsorbate thermal wavelength is large and the long-range order of the sample may influence the adsorbate gas thermodynamics. It is hoped that the low-temperature measurements of the specific heat may provide answers to these questions.

VI. SUMMARY AND CONCLUSION

⁴He gas adsorbed in the grooves of single-wall carbon nanotube bundles has been treated as an interacting Bose gas in one dimension. It was found that this approximation

should be very accurate for all temperatures below 8 K. The interactions in the adsorbed gas are treated via the quantum virial expansion approach, and the second virial coefficient for the interacting gas was calculated. This information was used to calculate the specific heat of adsorbed ⁴He gas which was shown to be substantially influenced by interadsorbate interactions already at relatively low adsorbate linear densities (0.0331/Å). A qualitative agreement between the results obtained in this paper and those of exactly solvable 1D models is demonstrated.

ACKNOWLEDGMENTS

It is a pleasure to thank D. Jurman for stimulating discussions concerning exactly solvable 1D many-particle models and for bringing the author's attention to Ref. 14.

*Email address: asiber@ifs.hr

- ¹W. Teizer, R. B. Hallock, E. Dujardin, and T. W. Ebbesen, *Phys. Rev. Lett.* **82**, 5305 (1999).
- ²W. Teizer, R. B. Hallock, E. Dujardin, and T. W. Ebbesen, *Phys. Rev. Lett.* **84**, 1844(E) (2000).
- ³Y. H. Kahng, R. B. Hallock, E. Dujardin, and T. W. Ebbesen, *J. Low Temp. Phys.* **126**, 223 (2002).
- ⁴S. Talapatra, A. Z. Zambano, S. E. Weber, and A. D. Migone, *Phys. Rev. Lett.* **85**, 138 (2000).
- ⁵M. M. Calbi, M. W. Cole, S. M. Gatica, M. J. Bojan, and G. Stan, *Rev. Mod. Phys.* **73**, 857 (2001).
- ⁶M. Boninsegni, S.-Y. Lee, and V. H. Crespi, *Phys. Rev. Lett.* **86**, 3360 (2001).
- ⁷M. W. Cole, V. H. Crespi, G. Stan, C. Ebner, J. M. Hartman, S. Moroni, and M. Boninsegni, *Phys. Rev. Lett.* **84**, 3883 (2000).
- ⁸S. M. Gatica, M. J. Bojan, G. Stan, and M. W. Cole, *J. Chem. Phys.* **114**, 3765 (2001).
- ⁹A. Šiber, *Phys. Rev. B* **66**, 205406 (2002).
- ¹⁰G. Stan, M. J. Bojan, S. Curtarolo, S. M. Gatica, and M. W. Cole, *Phys. Rev. B* **62**, 2173 (2000).
- ¹¹A. Šiber and H. Buljan, *Phys. Rev. B* **66**, 075415 (2002).
- ¹²A. Šiber, *Phys. Rev. B* **66**, 235414 (2002).
- ¹³J. Petterson and O. Hjortsberg, *Hydrogen Storage Alternatives—A Technological and Economic Assessment* (Kommunikationsforskningsberedningen, Stockholm, 1999).
- ¹⁴M. A. Olshanetsky and A. M. Perelomov, *Phys. Rep.* **71**, 313 (1981); M. A. Olshanetsky and A. M. Perelomov, *ibid.* **94**, 313 (1983).
- ¹⁵E. H. Lieb and W. Liniger, *Phys. Rev.* **130**, 1605 (1963).
- ¹⁶E. H. Lieb, *Phys. Rev.* **130**, 1616 (1963).
- ¹⁷M. Girardeau, *J. Math. Phys.* **1**, 516 (1960).
- ¹⁸A. R. Janzen and R. A. Aziz, *J. Chem. Phys.* **107**, 914 (1997).
- ¹⁹J. Hone, B. Batlogg, Z. Benes, A. T. Johnson, and J. E. Fischer, *Science* **289**, 1730 (2000).
- ²⁰J. C. Lasjaunias, K. Biljaković, Z. Benes, J. E. Fischer, and P. Monceau, *Phys. Rev. B* **65**, 113409 (2002).
- ²¹R. L. Siddon and M. Schick, *Phys. Rev. A* **9**, 907 (1974).
- ²²K. Huang, *Statistical Mechanics* (Wiley, New York, 1963).
- ²³*Problems in Thermodynamics and Statistical Physics*, edited by P. T. Landsberg (Pion, London, 1971).
- ²⁴L. I. Schiff, *Quantum Mechanics* (McGraw-Hill, New York, 1968).
- ²⁵L. W. Bruch, M. W. Cole, and E. Zaremba, *Physical Adsorption: Forces and Phenomena* (Clarendon, Oxford, 1997).
- ²⁶G. Vidali and M. W. Cole, *Phys. Rev. B* **22**, 4661 (1980).
- ²⁷M. Bretz, J. G. Dash, D. C. Hickernell, E. O. McLean, and O. E. Vilches, *Phys. Rev. A* **8**, 1589 (1973).
- ²⁸M. K. Kostov, M. W. Cole, J. C. Lewis, P. Diep, and J. K. Johnson, *Chem. Phys. Lett.* **332**, 26 (2000).
- ²⁹Z.-C. Guo and L. W. Bruch, *J. Chem. Phys.* **77**, 1417 (1982).
- ³⁰S. Kilić and L. Vranješ, *Croat. Chem. Acta* **73**, 517 (2000).
- ³¹L. Vranješ and S. Kilić, *Phys. Rev. A* **65**, 2506 (2002).
- ³²R. G. Gordon, *J. Chem. Phys.* **51**, 14 (1969).
- ³³M. E. Portnoi and I. Galbraith, *Phys. Rev. B* **58**, 3963 (1998).
- ³⁴Q.-G. Lin, *Phys. Rev. A* **56**, 1938 (1997).
- ³⁵N. Levinson, *K. Dan. Vidensk. Selsk. Mat. Fys. Medd.* **25**, 3 (1949).
- ³⁶M. W. Cole, D. R. Frankl, and D. L. Goodstein, *Rev. Mod. Phys.* **53**, 199 (1981).
- ³⁷J. J. Rehr and M. Tejwani, *Phys. Rev. B* **20**, 345 (1979).
- ³⁸J. G. Dash, *J. Low Temp. Phys.* **1**, 173 (1969).
- ³⁹R. L. Elgin and D. L. Goodstein, *Phys. Rev. A* **9**, 2657 (1974).
- ⁴⁰C. E. Campbell, J. G. Dash, and M. Schick, *Phys. Rev. Lett.* **26**, 966 (1971).